Pergamon

Int. J. Heat Mass Transfer. Vol. 39, No. 1, pp. 69–79, 1996
Elsevier Science Ltd
Printed in Great Britain

0017-9310(95)00100-X

Transient heat transfer in a semitransparent radiating layer with boundary convection and surface reflections

ROBERT SIEGEL
NASA Lewis Research Center, Cleveland, OH 44135, U.S.A.

(*Received* 15 *July* 1994 *and in final form* 17 *February* 1995)

Abstract Surface convection and refractive index effects are examined during transient radiative heating or cooling of a grey semitransparent layer with internal absorption, emission and conduction. Each side of the layer is exposed to hot or cold radiative surroundings, while each boundary is heated or cooled by convection. Emission within the layer and internal reflections depend on the layer refractive index. The reflected energy and heat conduction distribute energy across the layer and partially equalize the transient temperature distributions. Solutions are given to demonstrate the effect of radiative heating for layers with various optical thicknesses, the behavior of a layer heated by radiation on one side and convectively cooled on the other, and a layer heated by convection while being cooled by radiation. The numerical method is an implicit finite difference procedure with non-uniform space and time increments. The basic method developed in earlier work is expanded to include external convection and incident radiation.

INTRODUCTION

Thermal protection coatings and ceramic components are being developed for use at high temperatures in aircraft and automotive engines. They can be subjected to transient heating or cooling by a variety of external radiation and convection conditions. Some of the materials are partially transparent to radiative energy. Within the material radiative transport acts in combination with heat conduction. Since the materials operate at high temperatures there is considerable internal emission which is proportional to the layer refractive index squared. Ceramic refractive indices range from approximately 1.5 to 3 so internal radiation fluxes can be large. Since these fluxes depend strongly on temperature level, accurate instantaneous temperature distributions must be calculated during a transient numerical solution or the heat flows, and hence the solution will become inaccurate as time advances.

For semitransparent materials the transient thermal behavior of single and multiple plane layers, cylinders, spheres and a square geometry has been examined in the literature for a variety of radiative conditions. Compared with steady state, transient behavior has been studied to a much smaller extent. Two of the early transient studies [1, 2] are for a semitransparent layer bounded by walls at specified temperatures. The temperature of one wall is suddenly changed to initiate the transient. Index of refraction effects are not included so results apply for a gas with a refractive index of one. In a more recent work [3] transient temperatures in glass were analyzed by using a zonal type of method. Computations were made for a variety of conditions. Some results are for a layer confined between opaque walls with specified temperatures, others are for layer assumed to have opaque surfaces with temperatures that depend on external conditions. A few comments are made on the effects of increasing the layer refractive index from 1.5 (typical for glass) to 3.0. A cylindrical geometry is analyzed in ref. [4]; transient cooling characteristics are obtained for the cylinder exposed to a cold rarefied environment. A multilayered geometry is analyzed in ref. [5]. Transient cooling of a layer of liquid drops was investigated in ref. [6] relative to the design of a radiator to dissipate energy in outer space. The layer cools in the cold vacuum of space and does not have boundary convection or incident radiation. A particular solution was obtained in ref. [7] for cooling a layer by radiative loss in the limit of zero heat conduction. Transient radiative cooling of a two-dimensional square geometry with a refractive index of one was calculated in ref. [8] by a finite difference method.

The finite difference procedure that is a foundation for the present work was developed in refs. [9, 10]. In ref. [9] transient cooling was examined for a semitransparent material with a refractive index of one. The method was extended in ref. [10] to larger refractive indices that provide internal reflections. In refs. [9, 10] the layer was initially hot and was cooled by exposure to a cold vacuum environment. The present work includes radiative and convective heating or cooling on each boundary. The layer temperature is initially uniform. As the transient begins, the boundary regions can be heated or cooled rapidly depending on the external radiation and/or convection conditions. To account for large temperature variations

NOMENCLATURE

a absorption coefficient of layer [m^{-1}]
c specific heat of radiating medium [W s kg^{-1} K^{-1}]
D thickness of radiating layer [m]
$E_1 \ldots, E_n$ exponential integral functions
h convective heat transfer coefficient [W m^{-2} K^{-1}]
H convection radiation parameter, $h/\sigma T_i^3$
k thermal conductivity of layer [W m^{-1} K^{-1}]
n refractive index of layer
N conduction radiation parameter, $k/4\sigma T_i^3 D$
q heat flux [W m^{-2}]
$\tilde{q}$ dimensionless flux, $q/\sigma T_i^4$
q_r radiative heat flow per unit area and time [W m^{-2}]
q_{r1}, q_{r2} external radiative fluxes incident on sides of layer [W m^{-2}]
R radiative source term in energy equation
t dimensionless temperature, T/T_i
T absolute temperature [K]
T_i initial temperature of semitransparent layer [K]
T_m integrated mean temperature [K], $t_m = T_m/T_i$
T_s temperature of surroundings [K], $t_s = T_s/T_i$
x coordinate in direction across layer [m]
X dimensionless coordinate, x/D.

Greek symbols
ε_{ut} emittance for layer at uniform temperature
θ time [s]
κ_D optical thickness of layer, aD
ρ density of layer [kg m^{-3}]; surface reflectivity
σ Stefan Boltzmann constant [W m^{-2} K^{-4}]
τ dimensionless time, $(4\sigma T_i^3/\rho c D)\theta$.

Subscripts
a, b, c, d interfaces of layer, Fig. 1
g gas for convection at boundary
i initial condition; incoming radiation
i the ith X location
M total number of X grid points
n at the nth time increment
o outgoing radiation
s surrounding environment
ss at steady state
ut uniform temperature condition
1, 2 external conditions at two sides of layer.

that may develop for some conditions, non-uniform increments are used to concentrate grid points near the boundaries. Accurate surface temperatures must be obtained to prevent errors in the convective heat flows and in reradiation from the volume adjacent to the boundaries.

In the solution the radiative effect of the temperature distribution surrounding each location is integrated to obtain its contribution to the local absorbed energy within the medium. The transient energy equation is solved with an implicit finite difference procedure using this local radiative internal energy source that depends on the transient temperature distribution. Internal reflections have a large effect on the spatial distribution of absorbed energy. The boundary relations developed in earlier work are expanded to account for surface reflections, transmitted external radiation and convection.

ANALYSIS

Energy equation for transient cooling

A plane layer with thickness D, Fig. 1, is a gray emitting, absorbing and non-scattering material that is heat conducting and has a refractive index $n \geq 1$. Initially the layer is at a uniform temperature T_i so $t(X,0) = 1$. It is then placed in surroundings where it can receive diffuse radiant energy q_{r1} and q_{r2} on each side. The layer can also be cooled or heated on each

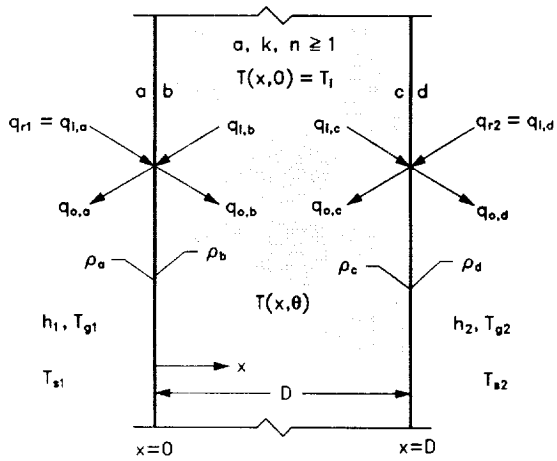

Fig. 1. Geometry, boundary conditions and nomenclature for plane layer with externally incident radiation and surface convection.

side by surrounding gas at temperatures T_{g1} and T_{g2} with heat transfer coefficients h_1 and h_2.

The transient energy equation in dimensionless form is [11]

$$\frac{\partial t}{\partial \tau} = N\frac{\partial^2 t}{\partial X^2} - R(t) \tag{1}$$

where $R(t)$ is the gradient of the radiative flux and is a function of X and τ

$$R(t) \equiv n^2\kappa_D t^4(X,\tau) - \frac{\kappa_D}{2}\left\{\tilde{q}_{o,b}(\tau)E_2(\kappa_D X) + \tilde{q}_{o,c}(\tau)E_2[\kappa_D(1-X)] + n^2\kappa_D\int_0^1 t^4(X^*,\tau)E_1(\kappa_D|X^*-X|)\mathrm{d}X^*\right\}. \tag{2}$$

The $\tilde{q}_{o,b}$ and $\tilde{q}_{o,c}$ are dimensionless diffuse fluxes that are outgoing from the internal sides of the layer boundaries (Fig. 1). They each consist of internally reflected energy and externally incident radiation transmitted through a boundary.

Boundary conditions

Boundary conditions are required for radiation and for heat conduction coupled with external convection. Radiation passes out of the layer from within the material; there is no emission at the boundaries which are planes without volume, hence there are no radiation terms in the surface convective boundary conditions. The conduction–convection boundary conditions at $x = 0$ and $x = D$ for all times are:

$$-k\left.\frac{\partial T}{\partial x}\right|_{x=0} = h_1[T_{g1} - T(x=0,\theta)] \tag{3a}$$

$$-k\left.\frac{\partial T}{\partial x}\right|_{x=D} = h_2[T(x=D,\theta) - T_{g2}]. \tag{3b}$$

The radiation boundary conditions are developed in a manner similar to refs. [10, 12]; they are required for the time-dependent fluxes $\tilde{q}_{o,b}(\tau)$ and $\tilde{q}_{o,c}(\tau)$ in equation (2). Using the reflectivities on both sides of the boundary surfaces, each $\tilde{q}_o$ is composed of transmitted and reflected portions: $\tilde{q}_{o,b} = (1-\rho_a)\tilde{q}_{r1} + \rho_b\tilde{q}_{i,b}$ and $\tilde{q}_{o,c} = (1-\rho_d)\tilde{q}_{r2} + \rho_c\tilde{q}_{i,c}$ (Fig. 1). The boundaries are assumed to be sufficiently rough that all reflections are diffuse; values of ρ are given in ref. [12]. The incident fluxes within the layer, $\tilde{q}_{i,b}$ and $\tilde{q}_{i,c}$, consist of energy leaving the opposite boundary and attenuated through the layer, and energy incident at the boundary as a result of emission within the layer. These are obtained from the radiative flux equation which is the integral of equation (2). As detailed in ref. [12],

$$\tilde{q}_{o,b}(\tau) = \frac{C_1(\tau) + A_b C_2(\tau)}{1 - A_b A_c} \tag{4a}$$

$$\tilde{q}_{o,c}(\tau) = \frac{C_2(\tau) + A_c C_1(\tau)}{1 - A_b A_c} \tag{4b}$$

where for conditions including incident external radiation

$$A_b = 2\rho_b E_3(\kappa_D) \tag{4c}$$

$$A_c = 2\rho_c E_3(\kappa_D) \tag{4d}$$

$$C_1(\tau) = (1-\rho_a)\tilde{q}_{r1} + 2n^2\rho_b\kappa_D\int_0^1 t^4(X,\tau)E_2(\kappa_D X)\mathrm{d}X \tag{4e}$$

$$C_2(\tau) = (1-\rho_d)\tilde{q}_{r2} + 2n^2\rho_c\kappa_D \times \int_0^1 t^4(X,\tau)E_2[\kappa_D(1-X)]\mathrm{d}X. \tag{4f}$$

For the specific case of black surroundings, $\tilde{q}_{r1} = t_{s1}^4$ and $\tilde{q}_{r2} = t_{s2}^4$.

Numerical solution procedure

To derive a transient solution method for equation (1), the numerical procedure in ref. [10] is used as a basis. A brief summary is given here with modifications for external radiation and convection. As shown in ref. [10], trapezoidal integration of $\partial t/\partial\tau$ over a small $\Delta\tau$ is used to advance the temperature an increment in time to give $\Delta t \equiv t_{n+1} - t_n \approx (\Delta\tau/2)[(\partial t/\partial\tau)_{n+1} + (\partial t/\partial\tau)_n]$. The second derivative of temperature at $\tau+\Delta\tau$ (at index $n+1$), is written in terms of $t(\tau)$ (at index n) and Δt as $(\partial^2 t/\partial X^2)_{n+1} = \partial^2\Delta t/\partial X^2 + \partial^2 t_n/\partial X^2$. The radiative source at $\tau+\Delta\tau$, $R(\tau+\Delta\tau) \equiv R_{n+1}$, is expressed in terms of $R(\tau) \equiv R_n$ by $R_{n+1} = R_n + (\partial R/\partial t)_n\Delta t$. By using equation (1) to eliminate $\partial t/\partial\tau$ in the Δt relation, and applying the two preceding relations in this paragraph, an equation for Δt is obtained:

$$\left[1 + \frac{\Delta\tau}{2}\left(\frac{\partial R}{\partial t}\right)_n - \frac{N\Delta\tau}{2}\left.\frac{\partial^2}{\partial X^2}\right|_n\right]\Delta t = \Delta\tau\left[N\left(\frac{\partial^2 t}{\partial X^2}\right)_n - R_n\right]. \tag{5}$$

The subscript i specifies the X location ($i = 1$ at $X = 0$, $i = M$ at $X = 1$). Relations are now developed to obtain $\Delta t(X_i) = \Delta t_i$ at the X_i at τ_n; the temperatures at τ_{n+1} are then $t_{n+1}(X_i) = t_n(X_i) + \Delta t(X_i)$. Since all terms on the right-hand sides of the preceding relations in this section are at τ corresponding to the index n, this subscript is omitted in the following.

To obtain a solution, relations are needed in equation (5) for $\partial^2/\partial X^2$ at the internal grid points of the layer and at the boundaries. For non-uniform increment sizes ΔX_i and $\Delta X_i'$ in the negative and positive directions about each X_i, the standard second derivative discretization is substituted into equation (5) to obtain an equation for Δt_i at the interior points $2 \leqslant i \leqslant M-1$.

$$-\frac{N\Delta\tau}{\Delta X_i\,(\Delta X_i^+ + \Delta X_i^-)}\Delta t_{i-1} + \left[1 + \frac{\Delta\tau}{2}\left(\frac{\partial R}{\partial t}\right)_i + \frac{N\Delta\tau}{\Delta X_i^+\,\Delta X_i^-}\right]\Delta t_i - \frac{N\Delta\tau}{\Delta X_i^+\,(\Delta X_i^- + \Delta X_i^+)}\Delta t_{i+1}$$

$$= \Delta\tau\left\{\frac{2N}{\Delta X_i^+ + \Delta X_i^-}\left[\frac{t_{i+1}}{\Delta X_i^+} - \left(\frac{\Delta X_i^- + \Delta X_i^+}{\Delta X_i^+\,\Delta X_i^-}\right)t_i + \frac{t_{i-1}}{\Delta X_i^-}\right] - R_i\right\}. \quad (6)$$

To account for convection at each boundary, equation (6) is replaced by special forms developed from the boundary conditions in equations (3a) and (3b). At $i = 1$, by using the definition of Δt, equation (3a) in dimensionless form $-\partial t/\partial X|_{i=1} = (H_1/4N)(t_{g1} - t_1)$ is written in terms of Δt by taking the difference in values at $\tau + \Delta\tau$ and τ:

$$\left.\frac{\partial \Delta t}{\partial X}\right|_{i=1} = \frac{H_1}{4N}\Delta t_1. \quad (7)$$

In the finite difference procedure the $\partial^2\Delta t/\partial X^2$ and $\partial^2 t/\partial X^2$ are needed at $i = 1$ for use in equation (5). Expanding for either $\xi = \Delta t$ or t about $i = 3/2$:

$$\left.\frac{\partial \xi}{\partial X}\right|_{i=3/2} = \left.\frac{\partial \xi}{\partial X}\right|_{i=1} + \left.\frac{\partial^2 \xi}{\partial X^2}\right|_{i=1}\frac{\Delta X_1^+}{2} + \ldots. \quad (8)$$

The quantity $(\xi_2 - \xi_1)/\Delta X_1^+$ is substituted in equation (8) for the first derivative at $i = 3/2$, and either equation (7) or equation (3a) is substituted for $\partial\Delta t/\partial X$ or $\partial t/\partial X$ at $i = 1$. After rearrangement,

$$\left.\frac{\partial^2 \Delta t}{\partial X^2}\right|_{i=1} = \frac{2}{\Delta X_1^+}\left[\frac{\Delta t_2 - \Delta t_1}{\Delta X_1^+} - \frac{H_1}{4N}\Delta t_1\right] \quad (9a)$$

$$\left.\frac{\partial^2 t}{\partial X^2}\right|_{i=1} = \frac{2}{\Delta X_1^+}\left[\frac{t_2 - t_1}{\Delta X_1^+} + \frac{H_1}{4N}(t_{g1} - t_1)\right]. \quad (9b)$$

For $i = 1$ substitute equations (9a) and (9b) into equation (5) to give, after rearrangement,

$$\left[1 + \frac{\Delta\tau}{2}\left(\frac{\partial R}{\partial t}\right)_1 + \frac{N\Delta\tau}{(\Delta X_1^+)^2}\left(1 + \frac{H_1\Delta X_1^+}{4N}\right)\right]\Delta t_1 - \frac{N\Delta\tau}{(\Delta X_1^+)^2}\Delta t_2$$

$$= \Delta\tau\left[\frac{2N}{(\Delta X_1^+)^2}(t_2 - t_1) + \frac{H_1}{2\Delta X_1^+}(t_{g1} - t_1) - R_1\right] \quad i = 1. \quad (10a)$$

Similarly, at $i = M$,

$$-\frac{N\Delta\tau}{(\Delta X_M)^2}\Delta t_{M-1} + \left[1 + \frac{\Delta\tau}{2}\left(\frac{\partial R}{\partial t}\right)_M + \frac{N\Delta\tau}{(\Delta X_M)^2}\left(1 + \frac{H_2\Delta X_M}{4N}\right)\right]\Delta t_M$$

$$= \Delta\tau\left[\frac{2N}{(\Delta X_M)^2}(t_{M-1} - t_M) + \frac{H_2}{2\Delta X_M}(t_{g2} - t_M) - R_M\right] \quad i = M. \quad (10b)$$

Equations (6) and (10) provide a tridiagonal system for obtaining $\Delta t_1, \Delta t_2 \ldots, \Delta t_M$; the coefficients are given in the Appendix.

$\partial R/\partial t$ is needed for the b_i coefficients. From equation (2):

$$\left.\frac{\partial R}{\partial t}\right|_X = 4n^2\kappa_D t^3(X,\tau) - \left[\frac{\kappa_D}{2}\left\{\frac{d\tilde{q}_{o,b}(\tau)}{d\tau}E_2(\kappa_D X) + \frac{d\tilde{q}_{o,c}(\tau)}{d\tau}E_2[\kappa_D(1-X)]\right\} + 2n^2\kappa_D^2 \times \int_0^1 t^3(X^*,\tau)\left.\frac{\partial t(X^*,\tau)}{\partial\tau}\right|_{X^*} E_1(\kappa_D|X^* - X|)dX^*\right] \times \left[\left.\frac{\partial t(X,\tau)}{\partial\tau}\right|_X\right]^{-1}. \quad (11)$$

From equation (4) the time derivatives of $\tilde{q}_{o,b}$ and $\tilde{q}_{o,c}$ in equation (11) are:

$$\frac{d\tilde{q}_{o,b}(\tau)}{d\tau} = \frac{(dC_1(\tau)/d\tau) + A_b(dC_2(\tau)/d\tau)}{1 - A_bA_c}$$

$$\frac{d\tilde{q}_{o,c}(\tau)}{d\tau} = \frac{(dC_2(\tau)/d\tau) + A_c(dC_1(\tau)/d\tau)}{1 - A_bA_c} \quad (12)$$

where

$$\frac{dC_1(\tau)}{d\tau} = 8n^2\rho_b\kappa_D\int_0^1 t^3(X,\tau)\left.\frac{\partial t(X,\tau)}{\partial\tau}\right|_X E_2(\kappa_D X)dX$$

$$\frac{dC_2(\tau)}{d\tau} = 8n^2\rho_c\kappa_D \times \int_0^1 t^3(X,\tau)\left.\frac{\partial t(X,\tau)}{\partial\tau}\right|_X E_2[\kappa_D(1-X)]dX.$$

The tridiagonal array is solved using the algorithm in refs. [13, 14]. At each X_i, Δt_i is added to t_i to advance the temperature to the next time.

To evaluate the radiative source term $R(t)$, equation (2), and its derivative $\partial R/\partial t$, equation (11), an accurate integration method is required. Special treatment as described in ref. [6] is used as X^* approaches X since $E_1(0) = \infty$. An analytical integration is used for a very small region about the singularity and Gaussian integration (using an IMSL subroutine) is used starting at this very small distance away from the singularity. Values of the functions at the unevenly spaced locations in the Gaussian subroutine are found from

the grid point values by cubic spline interpolation. By trying various ΔX values and numbers of grid points it was found that 50 increments across the layer gave accurate results for the κ_D considered here. Small values of $\Delta X = 0.1$ were used for 10 increments near the boundaries where temperature variations can be large. To avoid numerical instabilities that can arise for a complex integrodifferential equation as given by equations (1) and (2), a small time step $\Delta\tau = 0.005$ was used for the first $20\Delta\tau$; after that $\Delta\tau = 0.01$ was used. Typical computing times to reach $\tau = 2.0$ were 4 min on a Cray X-MP. In most instances the temperature distributions for $\tau = 1.5$ were less than 1% away from steady state.

Transient energy balance

The transient temperature distributions were used in an overall energy balance to check numerical solution accuracy at each time step. The instantaneous energy rate incident by radiation and added by convection is in dimensionless form, $\tilde{q}_{r1}+\tilde{q}_{r2}+H_1[t_{g1}-t(0,\tau)]+H_2[t_{g2}-t(1,\tau)]$. This must equal the sum of radiative energy reflected and emitted by the layer and the transient rate of energy storage. The reflected energy is $\rho_a\tilde{q}_{r1}+\rho_a\tilde{q}_{r2}$. The instantaneous radiative flux leaving through both boundaries is $(1-\rho_b)\tilde{q}_{i,b}+(1-\rho_c)\tilde{q}_{i,c}=[(1-\rho_b)/\rho_b][\tilde{q}_{o,b}-(1-\rho_a)\tilde{q}_{r1}]+[(1-\rho_c)/\rho_c][\tilde{q}_{o,c}-(1-\rho_d)\tilde{q}_{r2}]$. This was evaluated using $\tilde{q}_{o,b}$ and $\tilde{q}_{o,c}$ from equation (4). Note that in the limit when $n = 1$, $\rho_b = \rho_c = 0$ and $A_b = A_c = 0$; the ρ_b and ρ_c in the radiative flux calculation can then be removed algebraically to avoid singular behavior in the numerical calculations. The transient energy storage rate was obtained from $(4/\Delta\tau)[t_m(\tau+\Delta\tau)-t_m(\tau)]$ where $t_m(\tau)$ is the instantaneous integrated mean temperature across the layer. The overall energy balance was satisfied within 0.5% throughout the transient calculations.

Limit for infinite thermal conductivity

Some of the transient temperature distributions that will be given are for symmetric heat transfer conditions on both sides of the layer. For some values of the parameters the temperature distributions are somewhat uniform during a large portion of the transient. In the limit of infinite thermal conductivity the distribution is uniform at each time. It is of interest to compare this limiting solution with appropriate transient results.

For a gray layer at uniform temperature the layer emittance, which is equal to its absorptance, was derived in ref. [15] as

$$\varepsilon_{ut}(n,\kappa_D)=\alpha_{ut}(n,\kappa_D)=[1-\rho_a(n)]\frac{1-2E_3(\kappa_D)}{1-\left[1-\dfrac{1-\rho_a(n)}{n^2}\right]2E_3(\kappa_D)} \quad (13)$$

where $\rho_a(n)$ is given in ref. [12] from the Fresnel relations. For symmetric conditions $q_{r1} = q_{r2} \equiv q_{rs}$, $T_{g1} = T_{g2} \equiv T_g$, and $h_1 = h_2 \equiv h$. The transient energy balance of radiant absorption and emission, convection and internal energy storage is

$$\alpha_{ut}q_{rs}-\varepsilon_{ut}\sigma T_{ut}^4+h(T_g-T_{ut})=\rho c\frac{D}{2}\frac{dT_{ut}}{d\theta}. \quad (14)$$

The $\alpha_{ut} = \varepsilon_{ut}$ and equation (14) is placed in dimensionless form. The τ and t_{ut} variables are separated and the result integrated to yield the time corresponding to the transient temperature t_{ut}:

$$\tau(t_{ut})=2\int_{\xi=1}^{\xi=t_{ut}}\frac{d\xi}{\varepsilon_{ut}(\tilde{q}_{rs}-\xi^4)+H(t_g-\xi)}. \quad (15)$$

Values for $\varepsilon_{ut}(n,\kappa_D)$ are in refs. [10, 15]. Results from equation (15) are shown in some of the figures that follow and, where applicable, very good agreement is obtained with the transient finite difference solutions.

RESULTS AND DISCUSSION

The transient temperatures begin from a uniform initial temperature. For the results in Figs. 2–5, 7 and 8, the external radiation and convection conditions are symmetric on both sides of the layer so the transient temperatures are symmetric and the distributions are given for one-half of the layer. Results are given at five instances during the transient; the distribution for the largest time is at or very close to steady state. Some of the results for large time were checked with steady state calculations using the computer program from ref. [12]; excellent agreement was obtained.

Figures 2–5 give transient temperatures for a layer suddenly subjected on both sides to a higher temperature radiative environment so that $q_{r1} = \sigma T_{s1}^4 = q_{r2} = \sigma T_{s2}^4$, and to convective cooling. This could correspond to a film-cooled ceramic component exposed to a high heat flux from a soot filled flame. Figure 2(a)–(c) is for optical thicknesses $\kappa_D = 0.5$, 2 and 10. For $\kappa_D = 0.5$ the layer is somewhat optically thin, and radiation effects are limited by small absorption. For $\kappa_D = 2$ radiation can penetrate the entire layer, but there is significant absorption; this yields close to the maximum radiation effect throughout the layer. For $\kappa_D = 10$ the layer is somewhat optically thick and most absorption of external radiation is near the boundaries. During the transient the layer is heated on each side by black surroundings at a temperature 1.5 times the initial temperature ($\tilde{q}_{r1} = \tilde{q}_{r2} = 1.5^4$). Simultaneously the layer is cooled by gas on each side at $T_{g1} = T_{g2} = 0.5T_i$. The $H_1 = H_2 = 1$ parameters are such that convection is somewhat comparable with radiation. There is moderate conduction as given by the parameter $N = 0.1$. The solid curves are for a refractive index $n = 1$, the dashed curves are for $n = 2$.

In Fig. 2(a) where the layer is rather optically thin, external radiation passes readily into the interior to

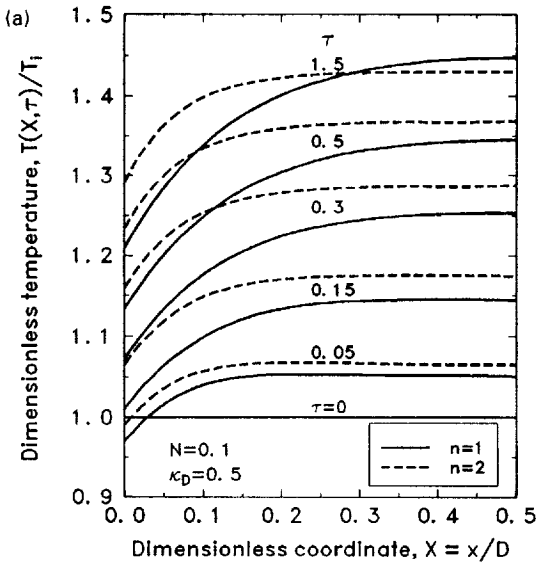

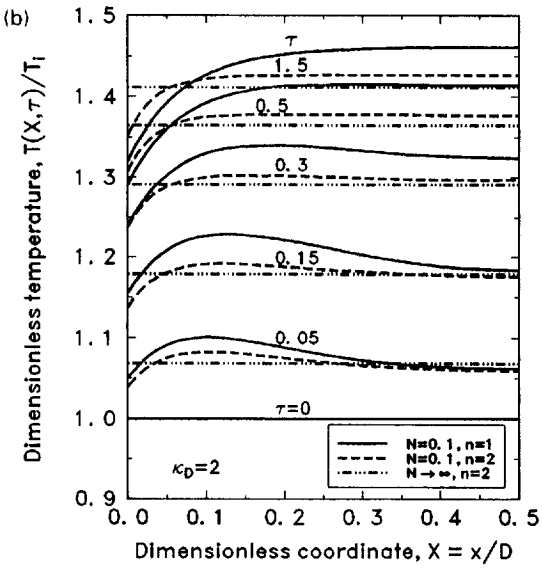

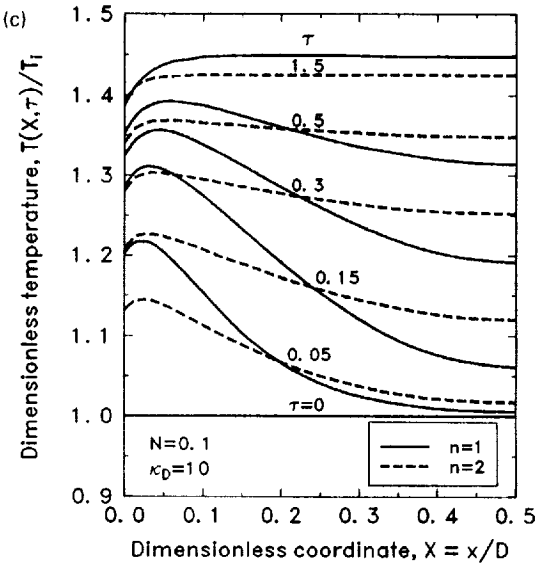

Fig. 2. Effect of refractive index on transient temperature distributions in a layer initially at uniform temperature, after exposure to external radiation and convective cooling. Parameters: $N = 0.1$, $\bar{q}_{r1} = \bar{q}_{r2} = 1.5^4$, $H_1 = H_2 = 1$, $t_{g1} = t_{g2} = 0.5$, $n = 1$ and 2. (a) Optical thickness $\kappa_D = 0.5$; (b) optical thickness $\kappa_D = 2$; (c) optical thickness $\kappa_D = 10$.

provide a fairly uniform internal heat source, some of which is removed by reradiation. Energy is removed near the wall by convection interacting with conduction. The result is that for small τ the interior temperature remains fairly uniform. As τ advances, the convection–conduction cooling penetrates the layer further and at the steady condition the profile has become somewhat parabolic as is typical for a layer with a uniform internal heat source. When the refractive index is increased from one to two the temperature profiles are more uniform. This is a result of increased radiative energy transfer across the layer arising from internal reflections. It is noted that for small τ the layer heats more rapidly when $n = 2$. This is caused by an increased layer absorptivity for small κ_D as shown in ref. [15].

The optical thickness is increased to $\kappa_D = 2$ in Fig. 2(b). It is more difficult for radiation to pass into the layer interior, and there is stronger absorption in the regions near the boundaries. For small τ this produces a maximum temperature at about $X = 0.1$. Heat is then conducted into the interior, and to the boundary where it is removed by convection. As τ increases, the interior temperature becomes more uniform as a result of conduction with lower radiation penetration; at steady state the temperature across most of the interior is much more uniform than in Fig. 2(a). Increasing n makes the temperature more uniform across the layer, but in contrast to Fig. 2(a) the layer heats more slowly. The horizontal dot–dash lines are for the limit of infinite conductivity from equation (15), and are for $n = 2$. Good agreement is obtained with the mean temperature levels of the dashed curves for $n = 2$.

The trends in Fig. 2(b) are accentuated in Fig. 2(c) where $\kappa_D = 10$. For a larger optical density of the layer, absorption of incident radiation occurs in regions closer to the surface and the temperature increases strongly in this region for small τ. Energy is transported into the interior by conduction and internal radiation, and the interior temperature distribution becomes uniform as steady state is approached. The surface temperature is reduced by convective cooling. There is a very significant effect of refractive index; the profiles for $n = 2$ are much more uniform.

Since the profiles have larger variations in shape when $n = 1$, results for $n = 1$ are used in Fig. 3 to illustrate further the effect of κ_D. Since the $N = 0.1$ parameter contains the layer thickness, D, it is best to think of all the results as being for the same D. The

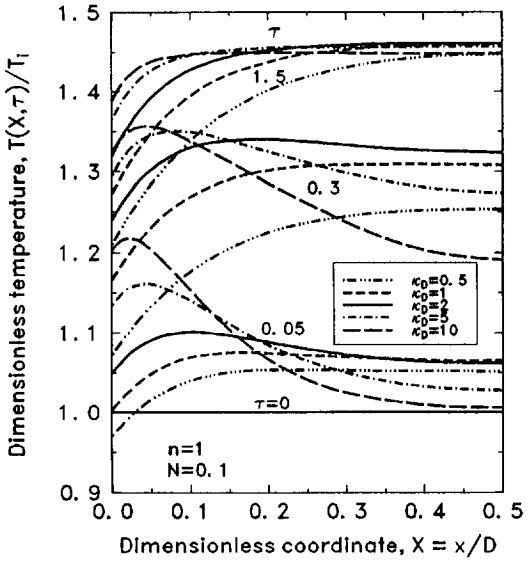

Fig. 3. Effect of optical thickness on transient temperature distributions during radiant heating and convective cooling of a layer with refractive index $n = 1$. Parameters: $N = 0.1$, $\tilde{q}_{r1} = \tilde{q}_{r2} = 1.5^4$, $H_1 = H_2 = 1$, $t_{g1} = t_{g2} = 0.5$.

κ_D is then changed by having materials with different absorption coefficients. With this viewpoint all of the results are for the same thermal conductivity. For $\tau = 0.05$ the results demonstrate the effect of increased radiant absorption near the boundary as κ_D increases. Near steady state, $\tau \approx 1.5$, increasing the optical density makes the temperatures almost uniform except near $X = 0$ within a region of decreasing width as κ_D increases.

Figure 4(a,b) shows the effect of the conduction parameter for $\kappa_D = 5$ and $n = 1$ and 2; the previous results were for $N = 0.1$. When N is increased to one in Fig. 4(a) the temperatures are fairly uniform throughout the transient. This is accentuated by increasing n to two in Fig. 4(b). The results approach the limiting horizontal lines from equation (15) for $N \to \infty$. For $N = 0.01$ and $n = 1$ there are substantial temperature gradients near the boundaries [Fig. 4(a)] from the interaction of strong radiant absorption and convective cooling. The gradients are substantially reduced for $n = 2$ in Fig. 4(b).

The effect of surface convection is demonstrated in Fig. 5 for $\kappa_D = 5$. Increasing $H_1 = H_2$ to five has a very strong effect throughout the transient. Large temperature gradients exist near the boundaries. Because of stronger cooling the steady state temperatures ($\tau \approx 1.5$), which represent a balance of radiative heating and convective cooling, are significantly reduced. Comparing Fig. 5(a) and (b) shows the effect of increasing n from one to two; for $n = 2$ the distributions are more uniform.

For Fig. 6 the conditions at the boundaries have been changed. The profiles are not symmetric and are shown for $X = 0$ to 1. The layer is heated on the

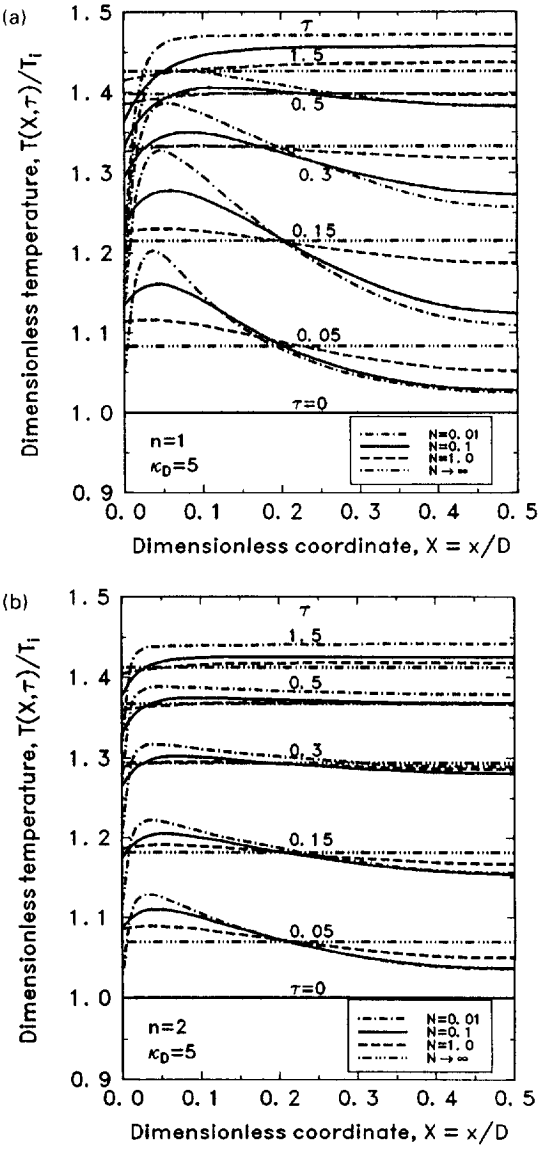

Fig. 4. Effect of conduction–radiation parameter on the transient temperature distributions in a layer during radiative heating and convective cooling starting from a uniform temperature for $\kappa_D = 5$. Parameters: $\tilde{q}_{r1} = \tilde{q}_{r2} = 1.5^4$, $H_1 = H_2 = 1$, $t_{g1} = t_{g2} = 0.5$. (a) Refractive index $n = 1$; (b) refractive index $n = 2$.

hot side by a radiative flux equal to that from black surroundings at $T_{s1} = 1.5T_i$. There is no convective cooling on the hot side, $H_1 = 0$; there is only reradiation on this side. Cooling occurs on the cold side ($X = 1$) by convection with $H_2 = 1$ and $T_{g2} = 0.5T_i$, and by radiation to black surroundings at $T_{s2} = 0.5T_i$. These conditions simulate heating a ceramic component by exposure on one side to a soot filled flame, and providing convective cooling only on the other side.

In Fig. 6(a) there is a large effect of increased refractive index in making the temperature distributions somewhat more uniform. At the hot side boundary the

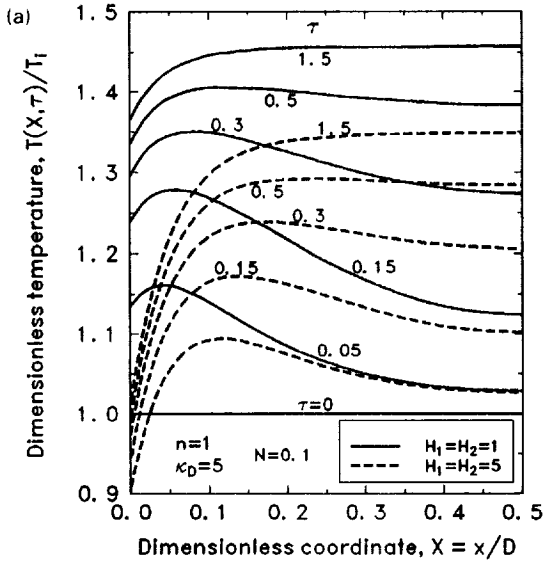

Fig. 5. Effect of external convection on transient temperature distributions in a layer during radiative heating and convective cooling starting from a uniform temperature for $\kappa_D = 5$. Parameters: $N = 0.1$, $\tilde{q}_{r1} = \tilde{q}_{r2} = 1.5^4$, $t_{g1} = t_{g2} = 0.5$. (a) Refractive index $n = 1$; (b) refractive index $n = 2$.

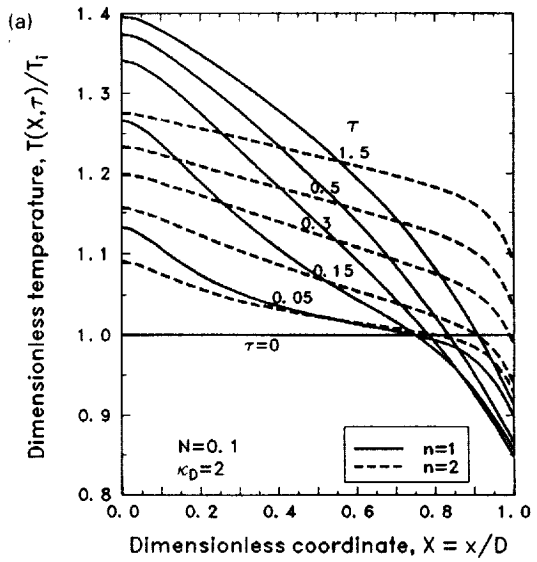

Fig. 6. Effect of refractive index on transient temperature distributions in a layer initially at uniform temperature after exposure to external radiation on one side without convective cooling on that side; cooling is by radiation and convection at the other side. Parameters: $N = 0.1$, $\tilde{q}_{r1} = 1.5^4$, $t_{s2} = 0.5$, $H_1 = 0$, $H_2 = 1$, $t_{g2} = 0.5$, $n = 1$ and 2. (a) Optical thickness $\kappa_D = 2$; (b) optical thickness $\kappa_D = 10$.

lack of convective cooling provides a zero temperature gradient since radiation leaves from within the volume and not from the surface itself. In Fig. 6(b) the κ_D is increased to 10 and there is more absorption of incident radiation near the hot boundary. Early in the transient there is a strong temperature rise near the hot boundary, while the temperatures decrease substantially at the boundary that is convectively cooled. Increasing n is not as effective in equalizing temperatures as in Fig. 6(a) because radiative transfer across the layer as augmented by internal reflections is reduced by the increased κ_D.

Another type of convection radiation interaction is illustrated by Figs. 7 and 8 where the layer is heated symmetrically by convection of a non-radiating hot gas. The radiative environment on both sides is cool, such as by having a surrounding film-cooled enclosure. At steady state, convective heating is balanced by radiative cooling from within the layer. Steady state temperatures as a function of κ_D are shown in Fig. 7(a) and (b) for $n = 1$ and 2. For $\kappa_D = 0$ there is no emission by the completely transparent layer, and convective heating on both sides with $t_{g1} = t_{g2} = 2$

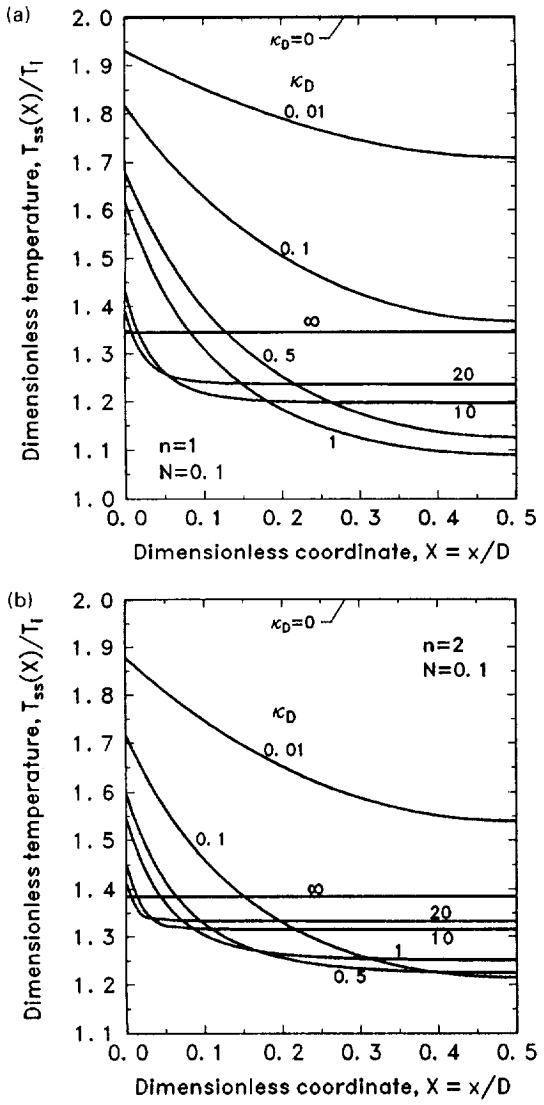

Fig. 7. Effect of optical thickness on steady state temperature distributions in a layer exposed to large convective heating while being cooled by radiation. Parameters: $N = 0.1$, $t_{s1} = t_{s2} = 0.2$, $H_1 = H_2 = 5$, $t_{g1} = t_{g2} = 2$. (a) Refractive index $n = 1$; (b) refractive index $n = 2$.

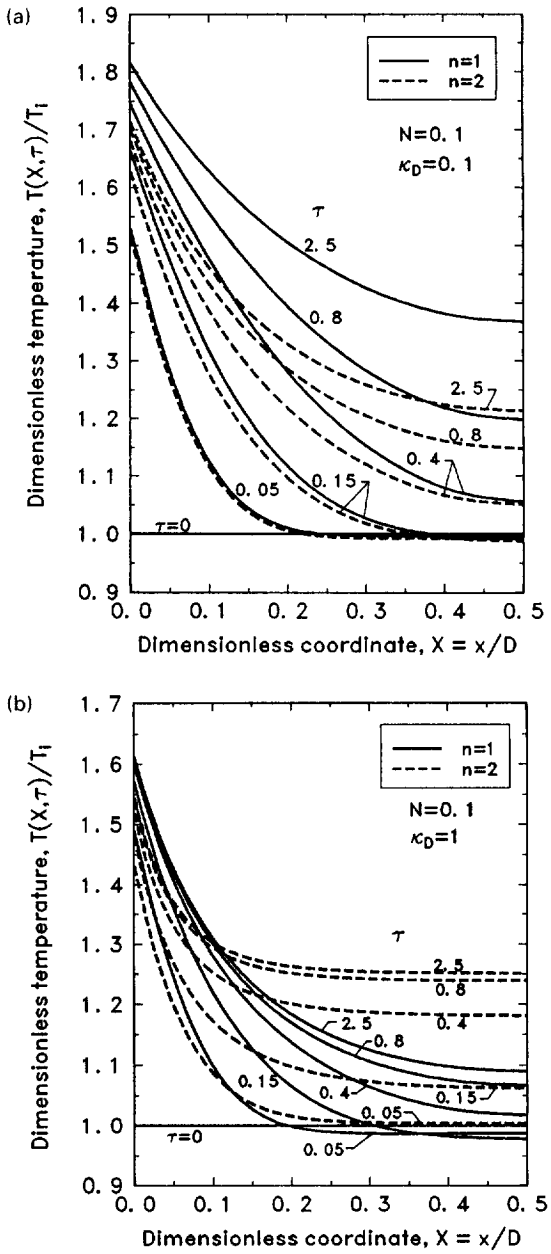

Fig. 8. Effect of refractive index on transient temperatures in a layer initially at uniform temperature after exposure to large external convective heating and radiative cooling. Parameters: $N = 0.1$, $t_{s1} = t_{s2} = 0.2$, $H_1 = H_2 = 5$, $t_{g1} = t_{g2} = 2$, $n = 1$ and 2. (a) Optical thickness $\kappa_D = 0.1$; (b) optical thickness $\kappa_D = 1$; (c) optical thickness $\kappa_D = 10$. (*Continued overleaf.*)

raises the temperature to $t_{ss} = 2$ throughout the layer. When $\kappa_D \to \infty$ the layer is opaque and the balance at the boundaries of convection, absorption and emission provides the uniform equilibrium temperature that is shown. For κ_D between these limits the results show the effect of internal radiative cooling on the steady state temperature distributions. For each κ_D the maximum temperatures are at the boundaries where convective heating is being applied, and the minimum temperature from radiative cooling is at the centerline. In Fig. 7(a) for $n = 1$, the lowest centerline temperature is for $\kappa_D \approx 1$. The lowest surface temperature is for an opaque layer. For $\kappa_D = 20$ the temperature distribution is flat over most of the layer, and radiation leaves from regions close to the boundaries. The results change somewhat in Fig. 7(b) where $n = 2$; for $\kappa_D > 0.5$ temperatures are more uniform in the central portion of the layer.

For three of the κ_D in Fig. 7, transient temperatures are shown in Fig. 8 for $n = 1$ and 2. The application of convective heating produces a rapid initial temperature rise near the boundary. In a few instances

(c)

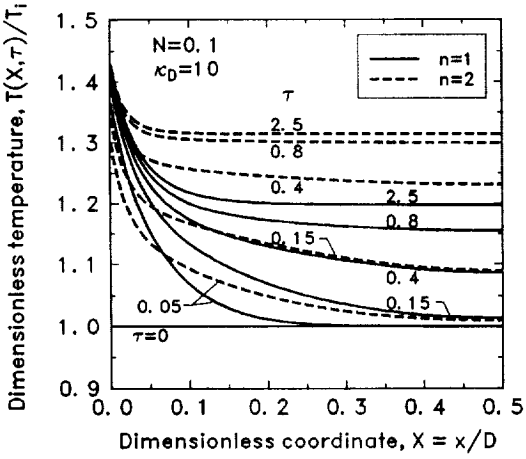

Fig. 8—*continued.*

radiative cooling produces temperatures in the central portion of the layer that are a little below the initial temperature. By comparing Fig. 8(a) and (b) it is evident that increasing κ_D and n provides more uniform temperature distributions. The effect of internal radiative cooling is substantial, as discussed for steady state results in Fig. 7.

CONCLUSIONS

Transient solutions are obtained for a semitransparent radiating and conducting layer heated or cooled by having each boundary exposed to radiation and/or convection. Results for $n = 1$ and 2 show the effect of the layer refractive index with boundary reflections assumed diffuse. A transient implicit finite difference formulation developed in previous work was extended to incorporate convective and radiative boundary conditions. Computing times on a Cray X-MP are about 4 min for a complete transient solution. The results at steady state were compared with solutions from a steady state analysis; excellent agreement was obtained.

To illustrate the radiative behavior and types of solutions that can be obtained, three types of transients are examined. For the first, a layer initially at uniform temperature is placed in a hot radiative environment while being cooled by convection at both boundaries. The transient temperature distributions can have rapidly varying shapes when the optical thickness is large so that absorption of incident energy is concentrated near the boundaries. An important effect of refractive index is that internal reflections promote the distribution of radiative energy within the layer; this makes the transient temperature distributions more uniform. For the second type of transient, the layer is heated by radiation on one side and is cooled by convection and radiation on the other. If the optical thickness is less than about 10, internal reflections provided by a refractive index of two have a substantial effect in equalizing the temperature distributions. For the third type of transient a layer in cold surroundings is subjected to heating on both sides by a hot transparent gas. While being heated the layer is losing energy by radiation. The minimum temperature is at the layer centerline, and the lowest steady state temperature is for $\kappa_D \approx 1$. For a large κ_D the temperatures are uniform over the central portion of the layer and the amplitude of the temperature variation is decreased.

REFERENCES

1. D. G. Doornink and R. G. Hering, Transient combined conductive and radiative heat transfer, *J. Heat Transfer* **94**, 473–478 (1972).
2. K. C. Weston and J. L. Hauth, Unsteady, combined radiation and conduction in an absorbing, scattering, and emitting medium, *J. Heat Transfer* **95**, 357–364 (1973).
3. T. H. Ping and M. Lallemand, Transient radiative conductive heat transfer in flat glasses submitted to temperature, flux and mixed boundary conditions, *Int. J. Heat Mass Transfer* **32**, 795–810 (1989).
4. S. W. Baek, T. Y. Kim and J. S. Lee, Transient cooling of a finite cylindrical medium in the rarefied cold environment, *Int. J. Heat Mass Transfer* **36**, 3949–3956 (1993).
5. C-F. Tsai and G. Nixon, Transient temperature distribution of a multilayer composite wall with effects of internal thermal radiation and conduction, *Numer. Heat Transfer* **10**, 95–101 (1986).
6. R. Siegel, Transient radiative cooling of a droplet-filled layer, *J. Heat Transfer* **109**, 159–164 (1987).
7. R. Siegel, Separation of variables solution for non-linear radiative cooling, *Int. J. Heat Mass Transfer* **30**, 959–965 (1987).
8. R. Siegel and F. B. Molls, Finite difference solution for transient radiative cooling of a conducting semitransparent square region, *Int. J. Heat Mass Transfer* **35**, 2579–2592 (1992).
9. R. Siegel, Finite difference solution for transient cooling of a radiating-conducting semitransparent layer, *J. Thermophys. Heat Transfer* **6**, 77–83 (1992).
10. R. Siegel, Refractive index effects on transient cooling of a semitransparent radiating layer, *J. Thermophys. Heat Transfer* **9**, 55–62 (1995).
11. R. Siegel and J. R. Howell, *Thermal Radiation Heat Transfer* (3rd Edn), Chap 14. Hemisphere, Washington, DC (1992).
12. C. M. Spuckler and R. Siegel, Refractive index effects on radiative behavior of a heated absorbing–emitting layer, *J. Thermophys. Heat Transfer* **6**, 596–604 (1992).
13. R. S. Varga, *Matrix Iterative Analysis*, p. 195. Prentice-Hall, Englewood Cliffs, New Jersey (1962).
14. W. H. Press, B. P. Flannery, S. A. Teukolsky and W. T. Vetterling, *Numerical Recipes*, pp. 40–41. Cambridge University Press, New York (1989).
15. R. Siegel and C. M. Spuckler, Effects of refractive index and diffuse or specular boundaries on a radiating isothermal layer, *J. Heat Transfer* **116**, 787–790 (1994).

APPENDIX: COEFFICIENTS FOR A TRIDIAGONAL SYSTEM

The tridiagonal system in equations (6) and (10) has the following coefficients:

$$\begin{bmatrix} b_1 & c_1 & & & \\ a_2 & \ddots & \ddots & & \\ & \ddots & \ddots & \ddots & \\ & & \ddots & \ddots & c_{M-1} \\ & & & a_M & b_M \end{bmatrix} \begin{bmatrix} \Delta t_1 \\ \Delta t_2 \\ \vdots \\ \Delta t_{M-1} \\ \Delta t_M \end{bmatrix} = \begin{bmatrix} s_1 \\ s_2 \\ \vdots \\ s_{M-1} \\ s_M \end{bmatrix}$$

$$a_i = -\frac{N\Delta\tau}{\Delta X_i^- (\Delta X_i^+ + \Delta X_i^-)} \quad 2 \leqslant i \leqslant M-1 \qquad a_M = -\frac{N\Delta\tau}{(\Delta X_M^-)^2}$$

$$b_1 = 1 + \frac{\Delta\tau}{2}\left(\frac{\partial R}{\partial t}\right)_1 + \frac{N\Delta\tau}{(\Delta X_1^+)^2}\left(1 + \frac{H_1 \Delta X_1^+}{4N}\right)$$

$$b_i = 1 + \frac{\Delta\tau}{2}\left(\frac{\partial R}{\partial t}\right)_i + \frac{N\Delta\tau}{(\Delta X_i^+ \Delta X_i^-)} \quad 2 \leqslant i \leqslant M-1$$

$$b_M = 1 + \frac{\Delta\tau}{2}\left(\frac{\partial R}{\partial t}\right)_M + \frac{N\Delta\tau}{(\Delta X_M^-)^2}\left(1 + \frac{H_2 \Delta X_M^-}{4N}\right)$$

$$c_1 = -\frac{N\Delta\tau}{(\Delta X_1^+)^2} \qquad c_i = -\frac{N\Delta\tau}{\Delta X_i^+ (\Delta X_i^+ + \Delta X_i^-)} \quad 2 \leqslant i \leqslant M-1$$

$$s_1 = \Delta\tau\left[\frac{2N}{(\Delta X_1^+)^2}(t_2 - t_1) + \frac{H_1}{2\Delta X_1^+}(t_{g1} - t_1) - R_1\right]$$

$$s_i = \Delta\tau\left\{\frac{2N}{\Delta X_i^+ + \Delta X_i^-}\left[\frac{t_{i+1}}{\Delta X_i^+} - \left(\frac{\Delta X_i^+ + \Delta X_i^-}{\Delta X_i^+ \Delta X_i^-}\right)t_i + \frac{t_{i-1}}{\Delta X_i^-}\right] - R_i\right\} \quad 2 \leqslant i \leqslant M-1$$

$$s_M = \Delta\tau\left[\frac{2N}{(\Delta X_M^-)^2}(t_{M-1} - t_M) + \frac{H_2}{2\Delta X_M^-}(t_{g2} - t_M) - R_M\right].$$